



PHOTONICS PUBLIC PRIVATE PARTNERSHIP



H2020-ICT-2019-2

Photonics Manufacturing Pilot Lines for Photonic Components and Devices

MedPhab

Photonics Solutions at Pilot Scale for Accelerated Medical Device Development

Starting date of the project: 01/01/2020

Duration: 48 months

= Deliverable D3.13 =

Dissemination material on in-vivo diagnostics (MODEL CASES)

Due date of deliverable: 31/05/2021

Actual submission date: 27/05/2021

Responsible WPL: Sanna Aikio, WP3, VTT

Responsible TL: Jarkko Tuominen, VTT

Deliverable responsible: Roger Krähenbühl, CSEM

Revision: V1.0

Dissemination level		
PU	Public	x
PP	Restricted to other programme participants (including the Commission Services)	
RE	Restricted to a group specified by the consortium (including the Commission Services)	
CO	Confidential, only for members of the consortium (including the Commission Services)	



This project has received funding from the European Union's Horizon 2020 research and innovation programme under grant agreement No 871345.

AUTHOR

Author	Institution	Contact (e-mail, phone)
Grigorij Muliuk	Imec	Grigorij.muliuk@ugent.be
Roger Krähenbühl	CSEM	Roger.kraehenbuehl@csem.ch

DOCUMENT CONTROL

Document version	Date	Change
V0.1	20.5.2021	First full draft
V1.0	25.5.2021	Final version

VALIDATION

Reviewers	Validation date
Work Package Leader	Sanna Aikio 24.5.2021
Project Manager	Mariana Pacheco Blanco 27.5.2021
Coordinator	Jussi Hiltunen 25.5.2021

DOCUMENT DATA

Keywords	Pilot line technical dissemination, model-case, wearable sensor, blood components measurement
Point of Contact	Name: Roger Kraehenbuehl Partner: CSEM SA Address: Tramstrasse 99 CH-4132 Muttenz Phone: +41 61 690 6011 E-mail: roger.kraehenbuehl@csem.ch
Delivery date	24.5.20.21

DISTRIBUTION LIST

Date	Version	Recipients
26.05.2021	V1.0	Partners via owncloud, EC via portal

DISCLAIMER

Any dissemination of results reflects only the authors' view and the European Commission Horizon 2020 is not responsible for any use that may be made of the information Deliverable D3.13 contains.

Executive Summary

The vision of this MedPhab model-case is to miniaturize a non-invasive measurement method to analyse patient's blood components with a wearable device. Technology works with an invisible infrared light beam that looks into the skin and counts specific molecules by analysis of the absorption spectra (heat induced optical deflection). The developed solution is an integrated device using a photonic integrated chip (PIC) assembled with optical fibers. The targeted device features an innovative Mach-Zehnder Interferometer (MZI) design with high sensitivity on temperature, incorporating low loss silicon waveguide, grating couplers for optical input and output, backside processing and ultraviolet (UV)-replication technology for compact folded fiber assembling.

Key technologies were selected, developed, and further advanced, such as: electron beam (e-beam) lithography enabling fast prototyping on 220 nm or 400 nm silicon-on-insulator (SOI) components, and UV replication of polymers to realize wafer-scale, folded micro-optical interconnects for self-aligned fiber assembly. The developed prototype was characterized with electro-optical measurements.

As a result, prototypes of very compact MZI-PIC's were realized and their capability to detect temperature for wearable applications was proved. Thereby, a size reduction of 99% and an increase of mechanical stability was obtained. The following scheme shows the integrated MZI-PIC sensor assembled with optical fibers.

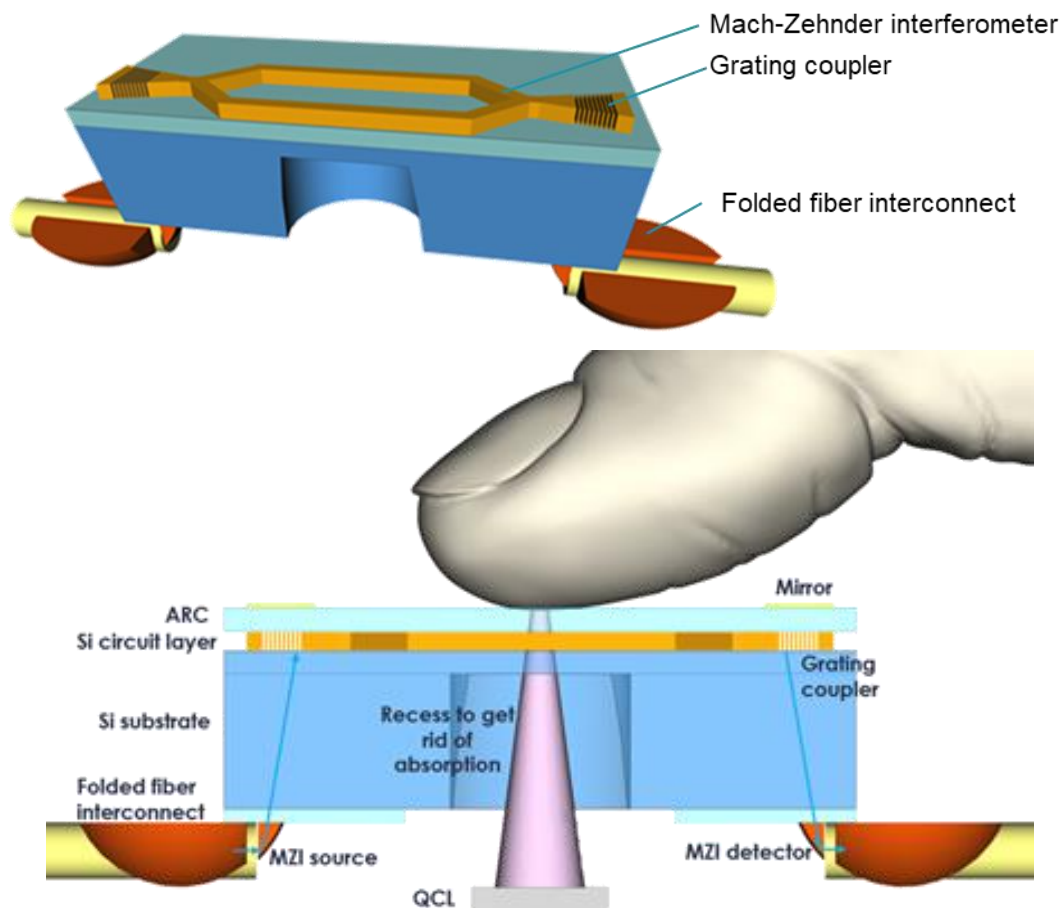


Table of Contents

1. Introduction	5
2. Results and Discussion.....	7
2.1. Design	7
2.1.1. MZI	7
2.1.2. Folded interconnect.....	9
2.2. Manufacturing	10
2.2.1. MZI-PIC	10
2.2.2. Folded interconnects	14
2.3. Characterization	14
2.3.1. Characterization method	14
2.3.2. Measurement results.....	15
2.3.3. Conclusions reflected against the set goals.....	16
2.4. Feasibility for wearable applications	16
3. Dissemination material.....	16
4. Conclusions	20
5. Degree of Progress	20
6. Dissemination Level.....	20

1. Introduction

The aim of the task T3.7 'Model cases' in the Work Package 3 'Production Acceleration' was to demonstrate and disseminate the pilot line capabilities through concrete example cases, and to develop pilot line ways of working.

The vision of the model-case 'Wearable PIC temperature sensor' is a medical device that non-invasively measures blood specific contents (i.e. glucose), without the need for a finger pricking, taking a blood sample or using a test strip. The ultimate goal is to miniaturize this in-vivo measurement approach (Figure 1) from the current shoebox size system, down to a wearable device. Preferred target is a hand wrist-watch-like gadget, which measures blood components (glucose) levels continuously.



Figure 1. Non-invasive blood component measurement approach: from shoebox size system to a handheld, and down to a wristwatch.

The blood components measurement technology works with an invisible infrared light beam that looks into the skin and counts specific molecules, by analysis of the absorption spectra (heat induced optical deflection). In particular, the idea is to replace the sensor (currently composed of conventional optical beam optics in conjunction with a crystal) by a photonic integrated chip (PIC) assembled with optical fibers (Figure 2).

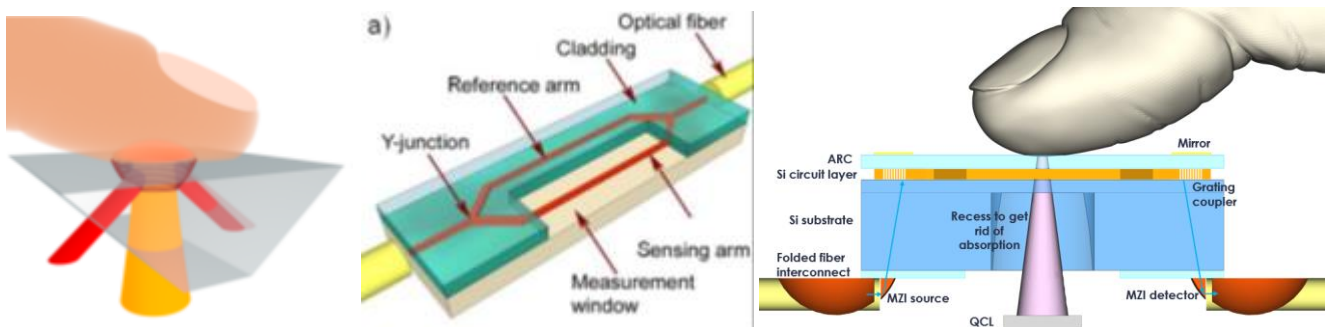


Figure 2. Current measurement sensor (left), the idea of an MZI-PIC (middle), and the cross section of the chosen folded fiber assembly (right).

The aim of this model-case was to prove the feasibility of an integrated PIC, that can detect temperature for a wearable application, and to realize a laboratory scale demonstrator using the capabilities of MedPhab consortium (Figure 3 and Figure 4). The specific goals were to a) reduce the size of the present system by more than 65%, and b) reduce the unwanted mechanical sensitivity by 50%, as the current crystal sensor is quite bulky (cm^3) and very sensitive to vibrations. The work was carried out by collaboration between Interuniversitair Micro-Electronica Centrum (IMEC) and CSEM Centre Suisse d'Electronique et de Microtechnique SA - Recherche et Developpement (CSEM).

In this report, the identified technological building blocks for PIC integration and system miniaturization are described, including a) MZI design with low loss silicon (Si) waveguide with high sensitivity on temperature (Section 2.1; page 7); b) grating couplers for optical in- and output; and c) silicon wafer backside processing and UV-replication technology for compact folded fiber assembly.

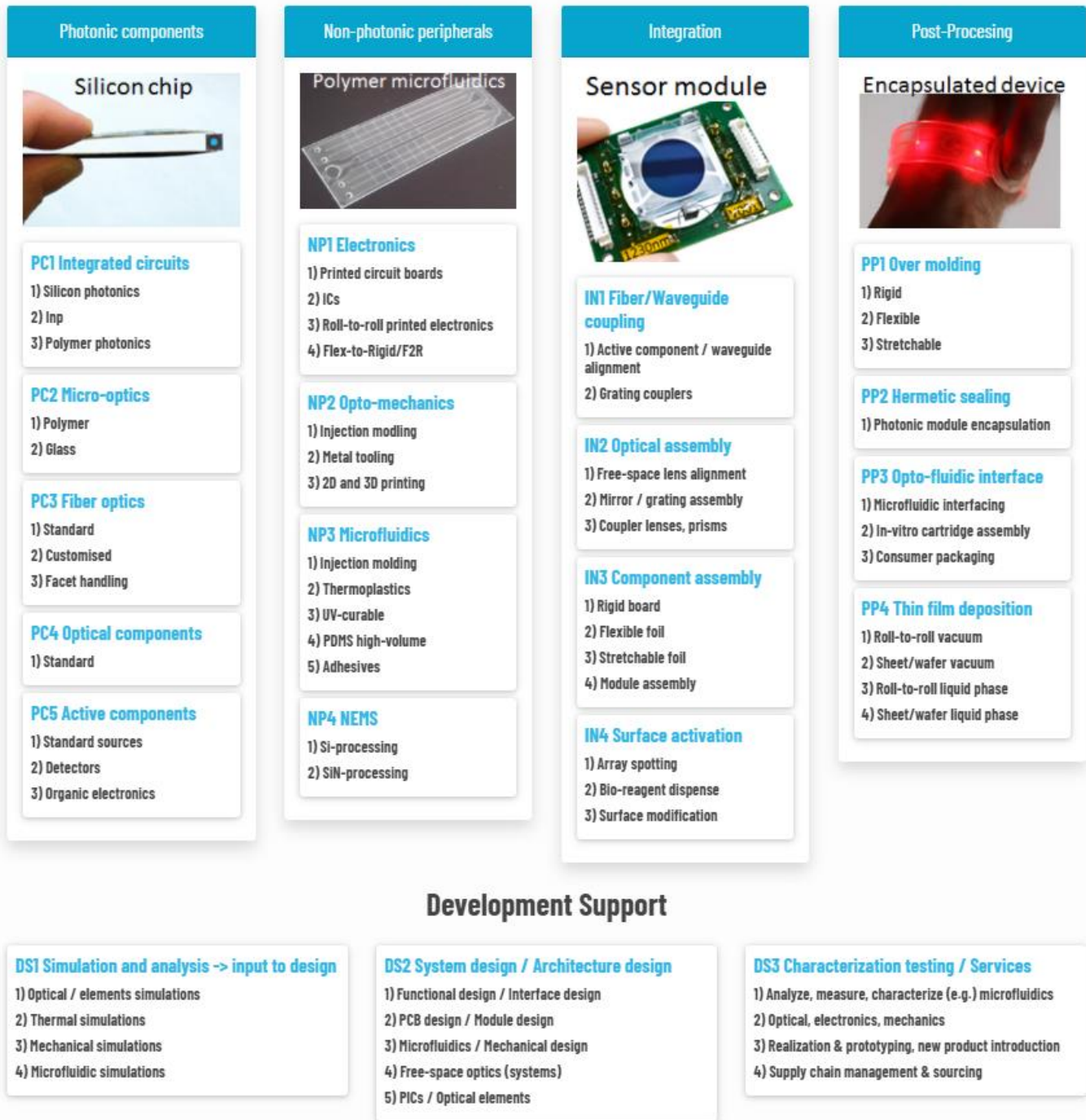


Figure 3. MedPhab's modularity table shows the pilot line technology offering in Photonic components, Non-photonic peripherals, Integration and Post-processing verticals and in Development support. These are further divided into technology modules that contain the processes.

Fabrication process

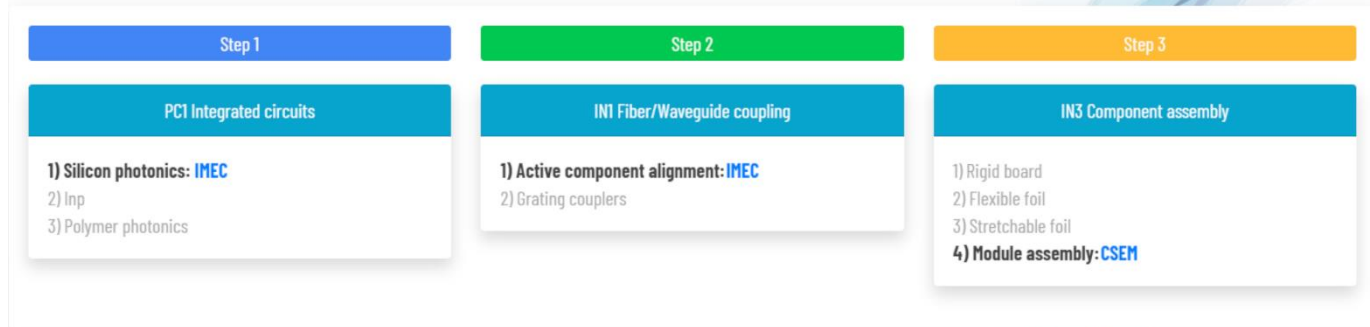


Figure 4. Production kit for the wearable temperature sensor. Production kit is a pre-defined collaboration between partners to accelerate the sensor realization and it is formed based on the pilot line Modularity table (Figure 3). The wearable temperature sensor is manufactured in three production steps by using the processes highlighted in the modules by the indicated partner.

2. Results and Discussion

IMEC took active part in the design and fabrication of the MZI-PIC-sensor. The key exploited technology was electron beam (e-beam) lithography enabling fast prototyping on 220 nm or 400 nm silicon-on-insulator (SOI) devices. In this work, we focused on less-mature e-beam lithography on 220 nm SOI.

Photonics packaging remains one the most challenging steps in the PIC industry. CSEM proposed to its “Wafer-scale Folded Micro-optical Interconnects”, as presented and published at ECOC2019¹, for coupling light from an optical fiber into the PIC. The technology is based on UV-replication into polymers, which produces smooth mirror surfaces and allows for “plug-and-play”-type components. In this work, CSEM focused on the feasibility to replicate these structures on top- or bottom-side of the grating couplers, but also on the optical characterization of the components and to prove the heat induced optical modulation of the MZI-PIC.

2.1. Design

2.1.1. MZI

The technical design of the MZI-sensor is displayed in Figure 5. We have an external 1550 nm probe laser, which sends the sensing light to the waveguide. This waveguide splits the light into a reference arm and to a sensing arm. The patient places his/her finger on the sensing arm (blue area in Figure 5). In this arm, there is a deeply etched hole from the backside and the stimulating light from a quantum cascade laser (QCL) interacts with the finger of the patient. This interaction affects to the sensing light propagation in the sensing arm by changing the refractive index n . The sensing light is combined with the reference light from the reference arm and the intensity of the outcoupled light is read-out by a photodetector. The photodetector is interfaced with the electronics block, which interprets the patient’s readings. The intensity modulation depth depends on the temperature sensitivity of the used waveguide material ($\Delta n/\Delta T$) and the sensing MZI arm length (Figure 5 right). With the used SOI waveguides, a longer than 1 mm MZI waveguide interaction length and an electronic lock-in amplification will allow detecting temperature changes in the mK range.

¹ R. Krähenbühl, A. Luu-Dinh and R. Ferrini, "Wafer-scale folded micro-optical interconnects," *45th European Conference on Optical Communication (ECOC 2019)*, 2019, pp. 1-3, doi: 10.1049/cp.2019.0916.

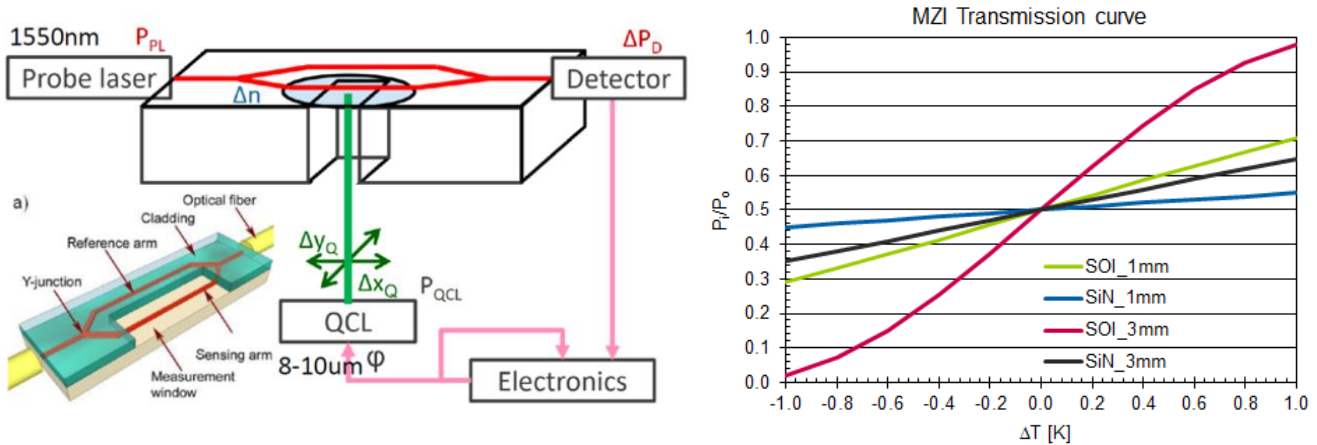


Figure 5. Left: Schematics of the MZI-sensor on silicon photonic PIC. Right: MZI transmission curve for various materials and MZI arm lengths (right).

During the designing of the MZI-sensor, a thorough parameter analysis was first made to study the possible sensor configurations. Based on this, we decided to pursue the basic idea displayed in Figure 6: circular sensing arm with the diameter d enabling finger placement, and reference arm spaced from the sensing arm by a distance g .

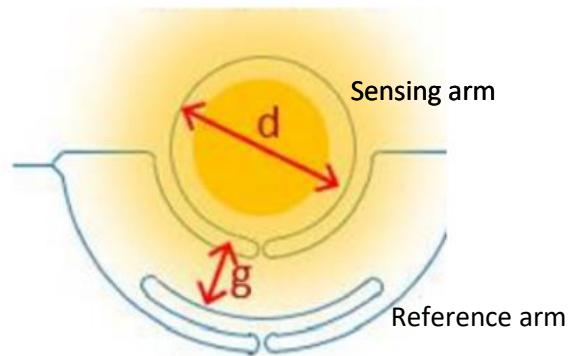


Figure 6. Envisioned MZI sensor design.

A parameter sweep was done in order to select a suitable sensor design for the application. An e-beam mask (Figure 7) was designed with a number of sensors with varying parameters: namely the sensing spot (d) was swept over 150, 300, 400, 500 μm ; the reference arm (g) was swept over 40, 80, 120 μm ; and the sensing length (L) was swept over 1350, 2100, 2600 and 3000 μm .

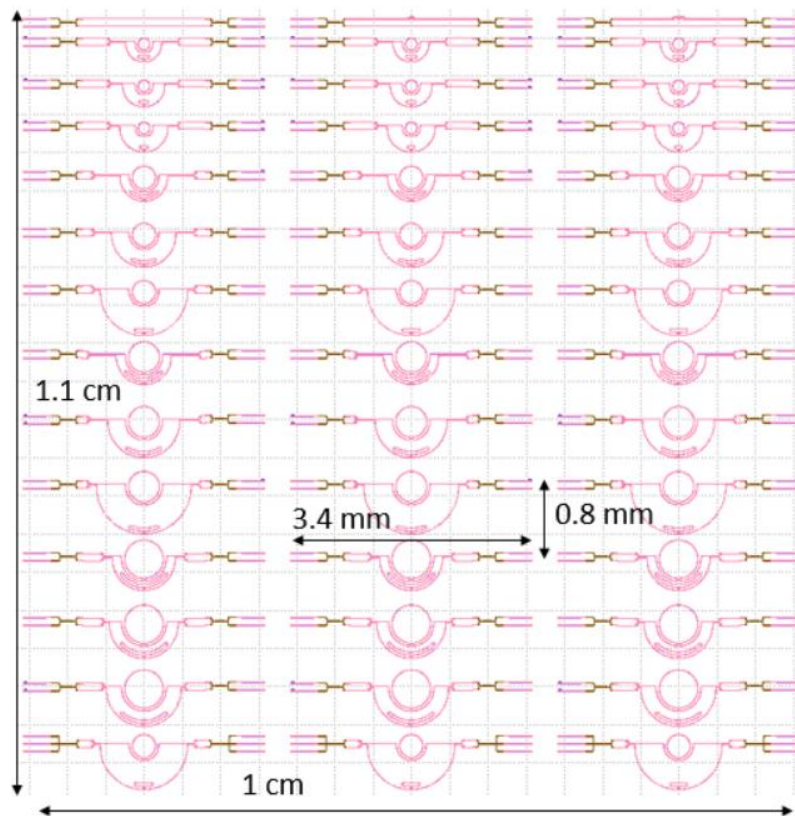


Figure 7. SOI e-beam mask design of MZI-sensors with different parameters to select the most suitable sensor design.

The mask, displayed in Figure 7, contains 36 different designs with same design used in each row with sweeps of delay line of $1\ \mu\text{m}$ (quasi-balanced), 10 and $20\ \mu\text{m}$ over column 1, 2 and 3, respectively. Each device is $3.4\ \text{mm}$ long and $800\ \mu\text{m}$ wide. In the design, we used a grating coupler optimized at $1550\ \text{nm}$ ($625\ \text{nm}$ period, 50% fill factor) for $220\ \text{nm}$ SOI. The total mask size including reference structures and excluding the alignment markers was $1.1\ \text{cm} \times 1\ \text{cm}$. We also designed reference waveguide structures as well as reference multimode interference (MMI) couplers and different waveguide spirals.

We explored two writing modes in patterning the structure: the standard and Fixed Beam Moving Stage (FBMS) mode. Difference between the modes is the movement of the sample stage and the electron gun. In the standard mode, the sample stage remains stationary while the electron gun moves. In the FBMS mode, the electron gun remains stationary while sample stage moves. We used the FBMS mode to define straight waveguides and linearly varying tapers, and to realise deep-etched ($220\ \text{nm}$) layers. The standard mode was used to define partially etched ($70\ \text{nm}$ deep) Si layers and MMI grating couplers. There is a limited movement of the gun in X- and Y-direction. Therefore, we had to take into account that the writing field of the e-beam in the standard mode is $500 \times 500\ \mu\text{m}$. Beyond that, stitching errors can appear, and we had to accommodate that by making waveguides wider in transitions.

2.1.2. Folded interconnect

The proposed compact folded interconnects are based on total internal reflection (TIR) and the design, as it is foreseen for the final MZI-PIC, is sketched in Figure 8. In the design of the folded micro-optical interconnects for $>90^\circ$ light redirection from a standard glass fiber, several constraints and requirements were taken into account. For example, the geometry of the micro-optical structures was designed to cover single mode fibers (SMF) on the input (SMFs E9, operating at $1550\ \text{nm}$ with a beam size of $10.5\ \mu\text{m}$ and a numerical aperture $\text{NA} = 0.13$), and multimode fibers on the output (MMFs G50, operating at $1550\ \text{nm}$ with a core size of $50\ \mu\text{m}$ and a numerical aperture $\text{NA} = 0.20$). Most important is that the height of the micro-optical elements must be compatible with the location and core size of the fibers. Further, the beam divergence at the exit of the glass fiber must comply with the TIR requirements at the reflecting optical interface.

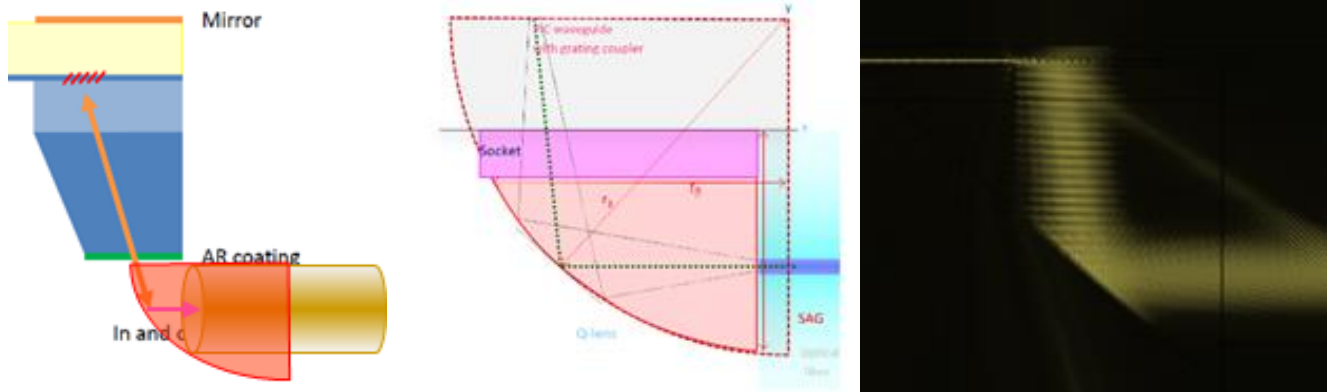


Figure 8. Folded micro-optical interconnects directly replicated on the back side of the MZI-PIC by UV imprint (left), beam divergence within the micro-optical element and main geometrical constraints for the SM fiber approach (middle), and corresponding beam propagation simulation (right).

While processing the micro-optical structures, self-alignment structures were replicated for passive fiber alignment (Figure 9). Here the design of the gap is crucial, as it has to be wide enough to accommodate the fiber inside and tight enough to have little alignment mismatch as possible.

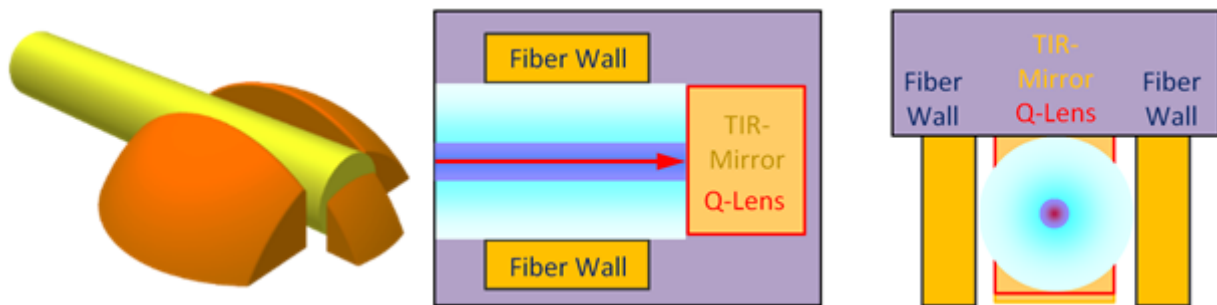


Figure 9. Sketches of the self-alignment structures for passive fiber alignment: 3D view (left), top view (middle), and front view (right).

2.2. Manufacturing

2.2.1. MZI-PIC

The schematic cross-section of the chip is displayed in Figure 10. For this cross-section, three important manufacturing steps had to be specified:

1. MZI mask fabrication using e-beam technology.
2. Backside alignment marker placement for backside etching/coupling scheme.
3. Backside light coupling scheme.

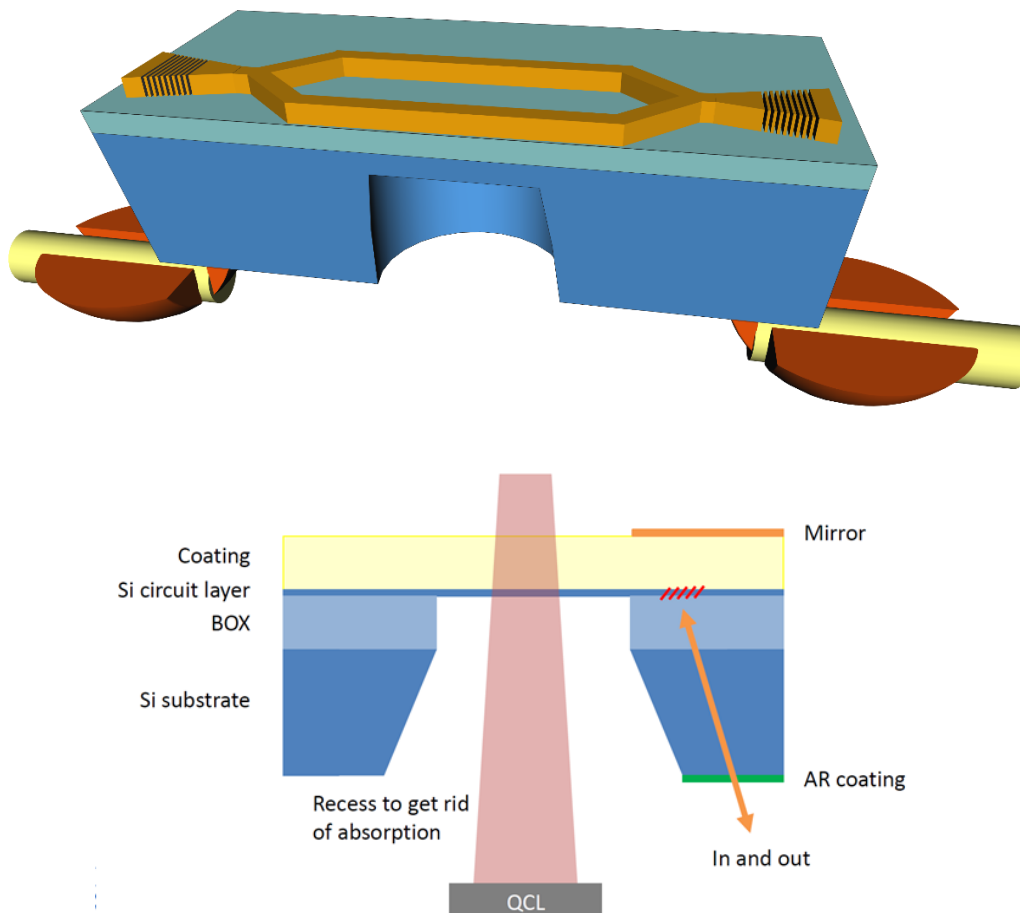


Figure 10. Schematic 3D view and cross-section of the fabricated SOI chip

The design described in Figure 5 has been fabricated using 220 nm SOI. The chip was patterned using e-beam lithography and reactive ion etching (RIE) cold plasma to etch 70 nm/220 nm top silicon layer. The manufacturing results are demonstrated in Figure 11. The transition between the FBMS and standard mode indicate no stitching errors or misalignment between the modes.

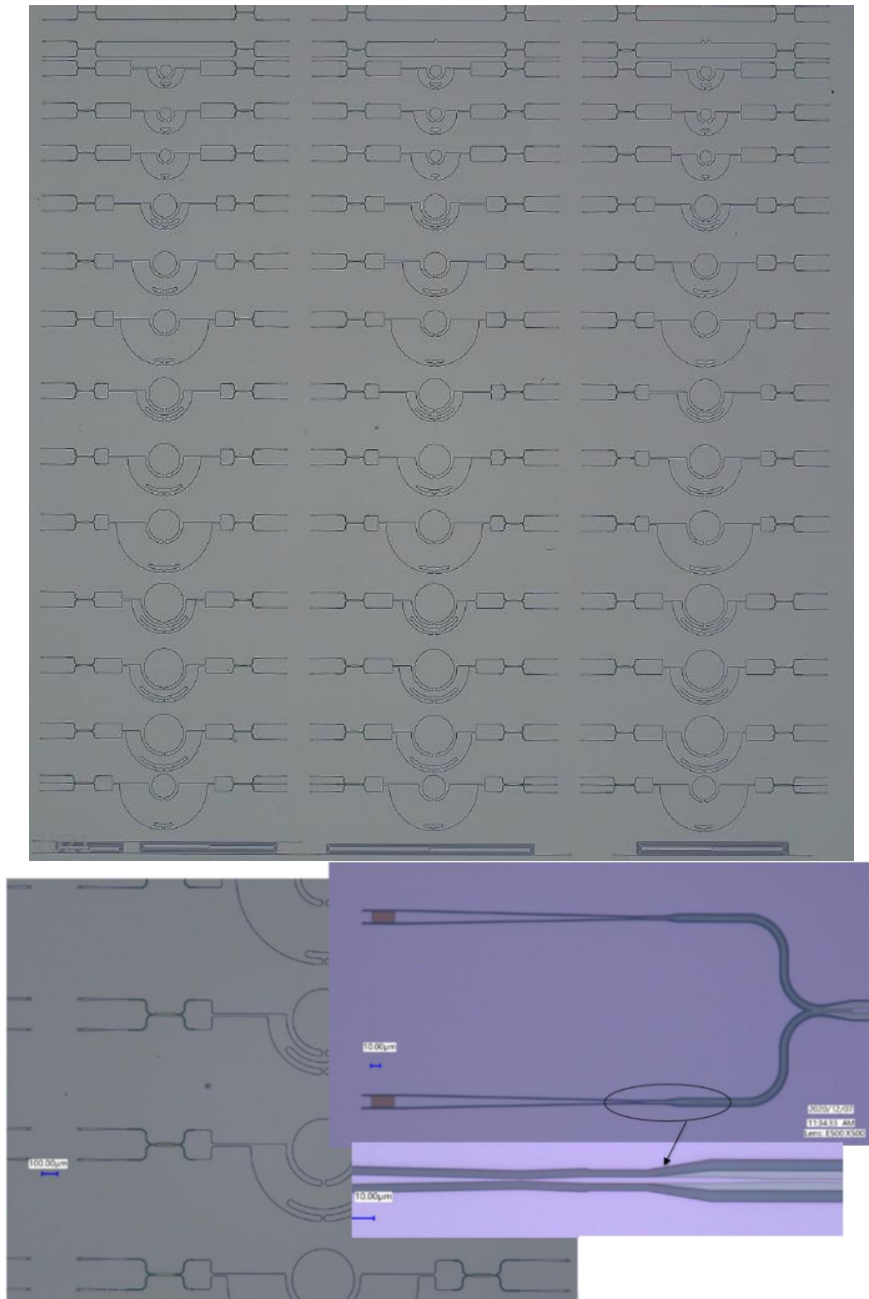


Figure 11. Microscope image of the fabricated SOI chip (top) using e-beam lithography. The inset (below) demonstrates a good transition between full-etch and partially-etched areas. In this work, it was important to develop a backside-coupling scheme, whereby the light propagating in the MZI Si waveguide can couple to the backside of the die. In addition, it was important to develop the backside etching mechanism (to develop a recess), in which QCL light can interact with a finger (see Figure 2). We patterned alignment markers on the front of the sample. Using the e-beam technology, it is also possible to pattern the alignment markers on the backside using the front side alignment markers.

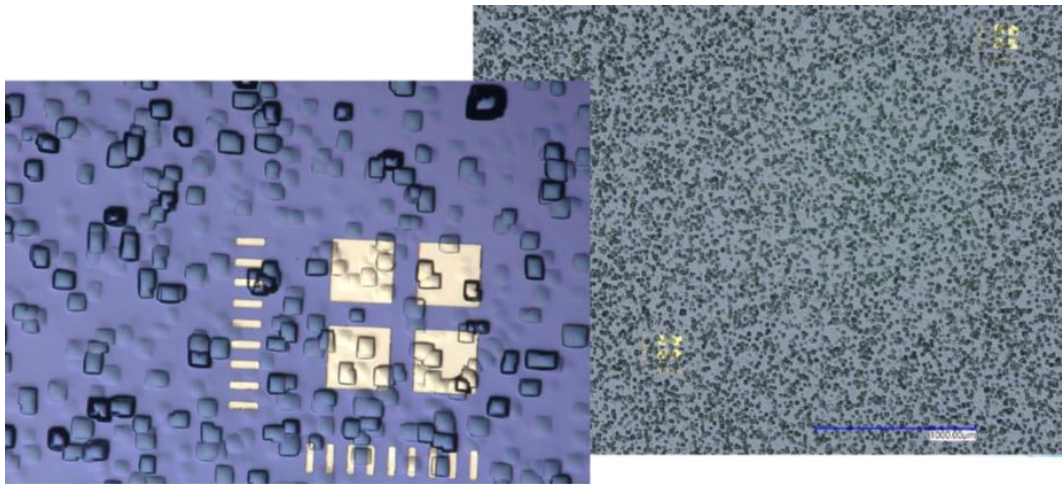


Figure 12. Gold alignment markers placed on the Si substrate.

The results are depicted in Figure 12. The gold (Au) markers are written on the backside of the die. The backside is not polished and therefore it looks grainy and non-smooth. Metal was used to increase the contrast for the post-processing. Two 220 nm SOI dies were sent by IMEC to CSEM to analyse the results of the process development.

The backside alignment method is shown in Figure 13. The coupling scheme makes use of the Ti/Al mirror, which constructively reflects the light to the bottom substrate, to be collected by a lensed optical fiber.

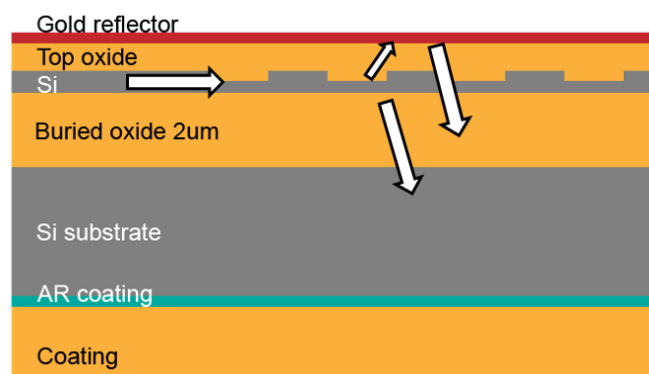


Figure 13. Simulated cross-section of the mirror.

IMEC performed simulations to find the optimal parameters for the mirror. The grating coupler was assumed to have a period of 625 nm with the 50% fill factor (FF) and 70 nm etched depth – we used the same grating coupler we fabricated using the e-beam run. In order to optimize the mirror, we had to find the top oxide thickness, which will lead to a constructive interference. We swept over the top oxide thicknesses (Figure 14a) to find the optimum at 200 nm and 650 nm. In addition, we had to include the antireflection (AR) coating to minimize the back-reflection between the silicon substrate and the polymer mirror. Here we approximated this material by SiOx. Simulation results shown at Figure 14b display that 200nm SiNx should be enough to prevent reflections. In other simulations, we considered the spot size, and in order to make it as small as possible for efficient coupling to the fiber, we had to thin the silicon substrate as much as possible. However, in order to handle the sample in the lab and to enable the sample shipping between locations, the substrate had to be rigid. Therefore, we did not grind the substrate thinner than 300 μm . Thus, the expected efficiency is lower.

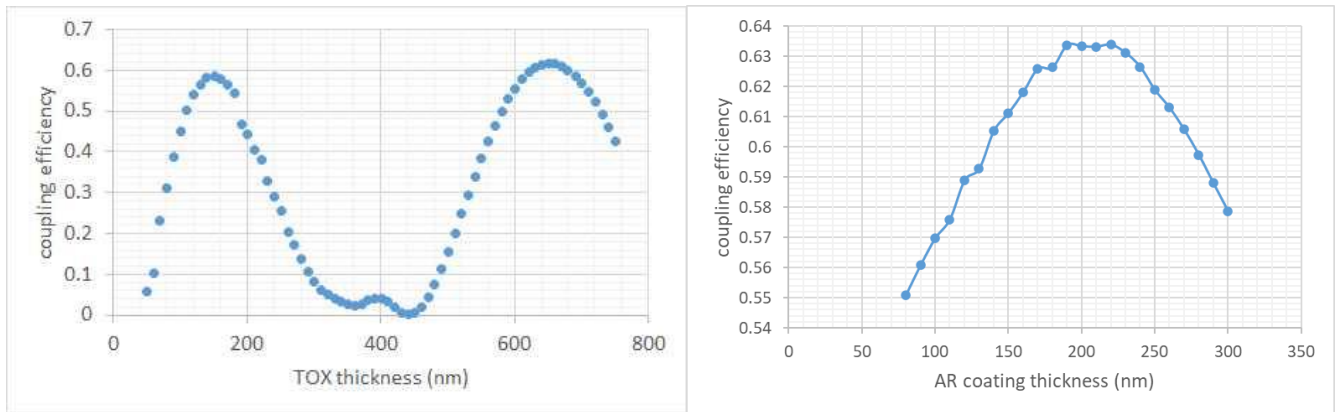


Figure 14. Simulation results of the top oxide thickness (left) and SiNx AR coating thickness (right).

2.2.2. Folded interconnects

One of the most cost-effective fabrication technologies for volume production of micro-optical components is based on UV wafer-scale replication into chemically stable polymers using standard semiconductor equipment. The process consists of two steps (Figure 15 left): First, the micro-optical structures are originated, and a master is fabricated, which is then used to produce the replication tool (mold). For the mastering of standard micro-lenses (i.e. Q-lenses), photolithography and a reflow process are applied. Second, the micro-optical elements are replicated into a UV curable polymer using the fabricated mold. In particular, for the UV casting process, we used a modified MA6 mask-aligner from Süss Microtec that enables the replication of micro-optical structures at wafer-level with a precise control of the alignment (below ± 1 microns) and of the height (± 2 microns) of the replicated elements. A residual layer (socket) both defines and precisely limits the achievable height.

As for the replication of the Q-lenses together with the self-alignment structures, the UV exposure is done through a specifically designed photomask that defines the final shape of the replicated structures on the PIC wafer. In that way we realized structures on glass, as well as on top of grating couplers (Figure 15 right).

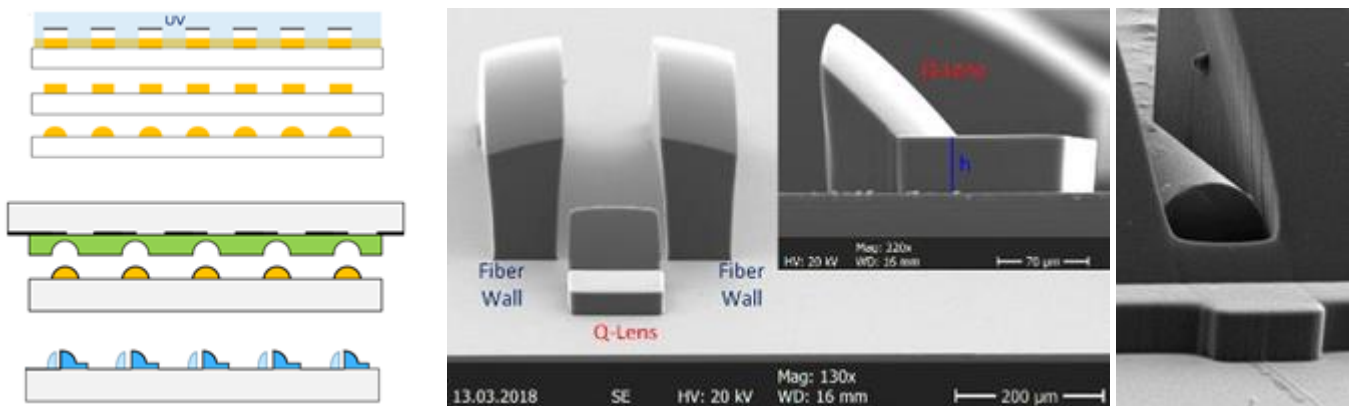


Figure 15. UV exposure through a photomask (left) to define the final shape of Q-lenses; self-alignment structures (middle) and a corresponding SEM image (right).

2.3. Characterization

2.3.1. Characterization method

CSEM has built for this model-case a flexible fiber optical measurement setup (Figure 16). For the measurement of the sensor heat dependence, an additional compact electrical thin wire can be placed in between of the two optical fibers. Applying a voltage signal will result in a heat signal.

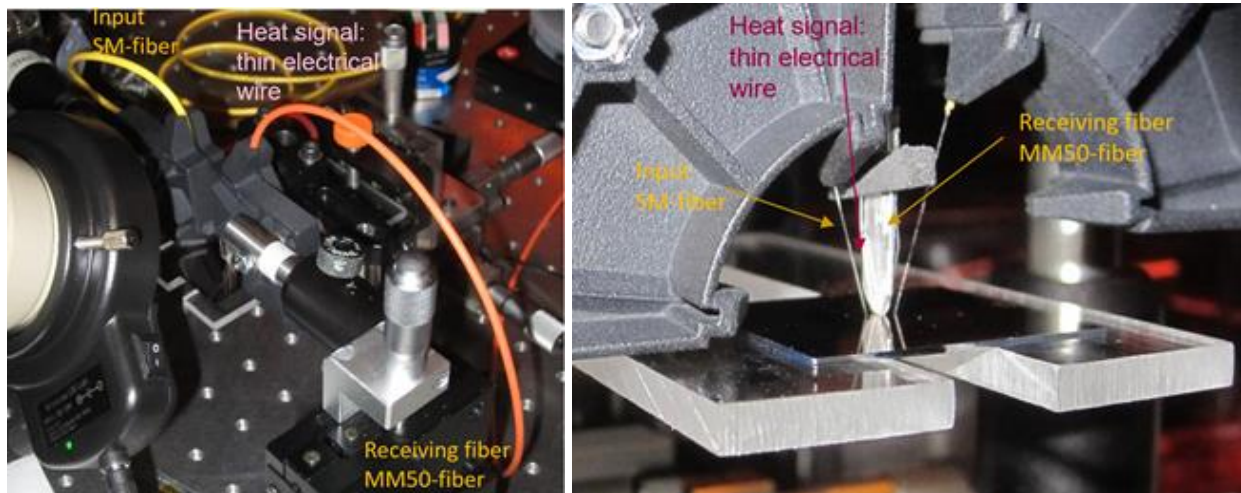


Figure 16. Optical characterization setup to measure the optical fiber-to-fiber losses, the beam profile at different propagation distances, and the optical response of the MZI-PIC in respect of heat change

The setup can handle most commercially available optical fiber types (SM E9, MM G50, H200, etc.) and cover a wide wavelength range (400nm - 1700nm, source and detector). It further can adjust angles (0-90 degree) of input and output fiber.

2.3.2. Measurement results

Using the above setup at CSEM, the optical fiber-to-fiber losses were determined. Using a $1.55 \mu\text{m}$ wavelength, a standard single mode fiber (E9) as input and a standard multimode fiber (G50) as output (configuration used for the sensing application), the optical losses for straight waveguides and MZI devices were measured.

For the first-generation devices, the losses were in the 16...20 dB range, whereas for the second-generation around 12...18 dB.

In order to assess the diffraction angle and beam divergence of the waveguide grating couplers, the horizontal (x-axis) beam profile was measured at different positions above the grating (z-axis). The resulting curves are shown in Figure 17. The evaluated diffraction angle was around 11 degrees.

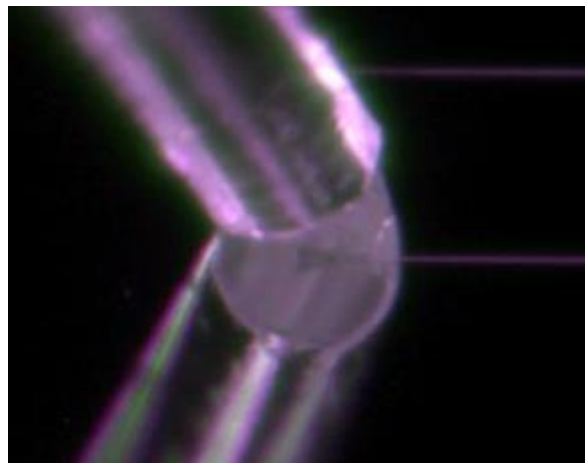
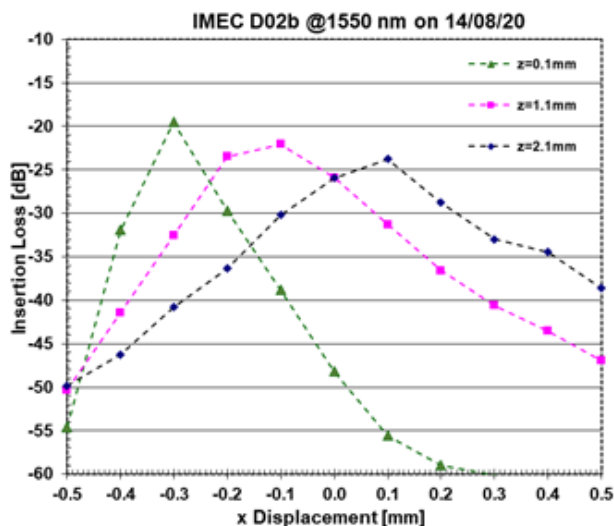


Figure 17. Optical transmission measurements of the beam profile at different height positions leading to a diffraction angle of 11 degrees (left); fiber on top of a grating coupler on the setup (right)

To finally prove the feasibility of the used MZI-PIC devices to be capable of detecting temperature for wearable applications, we introduced a heat source into the centre of the designated MZI arm using a thin electric wire between the two optical fibers (Figure 18 left), driven by an alternating (0 to 2V) electrical voltage signal. The resulting optical signals are shown in Figure 18 (right).

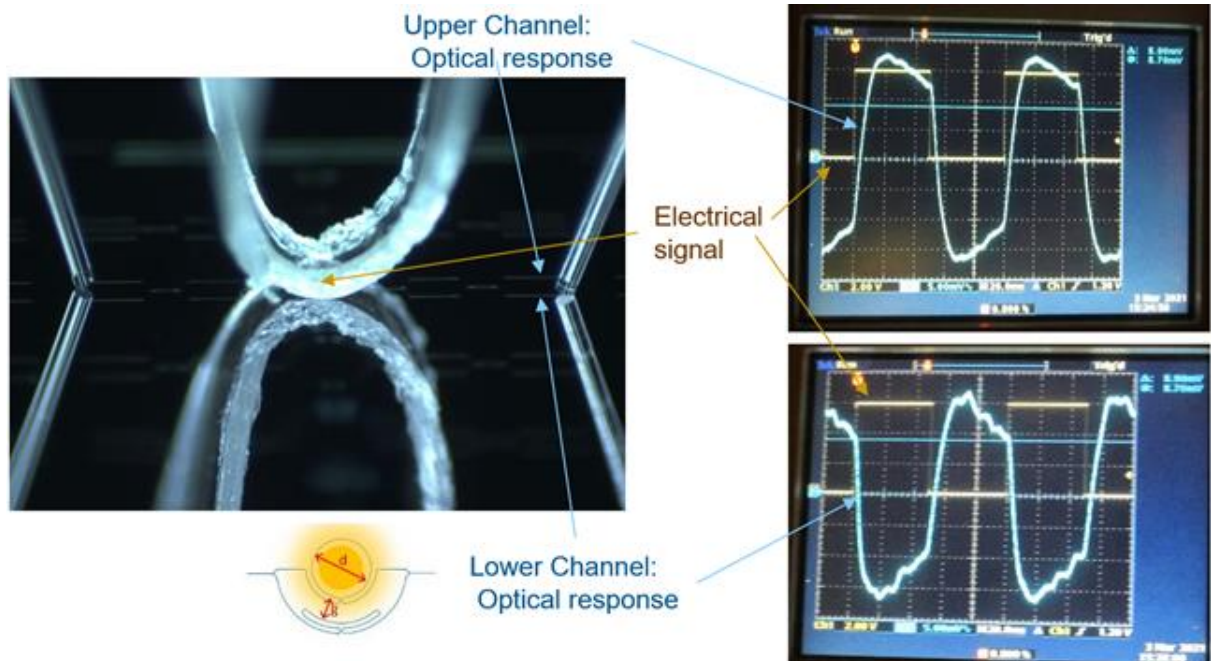


Figure 18. Optical characterization setup (left) and measurement results of the optical response of the two MZI output channels in respect of the electronic wire induced heat change (left).

The nice optical response following the electrical signal were an impressive result and proved the usability of the chosen MZI-PIC technology.

2.3.3. Conclusions reflected against the set goals

The MZI-PIC device (including the backside assembled fibers) has the size of around $3.7 \times 0.8 \times 1.0 \text{ mm}^3$. This is in the range of 1% of the initial crystal of 1 cm^3 (even without optics) and clearly below the aimed target of 65% size reduction.

As the final device would be fully assembled with optical fibers (leading to no mechanical movable parts), the device should be not sensitive at all to mechanical vibration, again fulfilling the set requirement of decreasing the mechanical instability by far more than 50%.

2.4. Feasibility for wearable applications

With the current approach, using optical fiber as optical in- and output, wearability is restricted to belt type devices. Thereby, active optical components, power source and detection system are decoupled from the sensing element, which is advantageous for the measurement accuracy, repeatability and reliability.

However, integration of all optical active components into a wristwatch type device is feasible. To reach this encouraging goal, the SM sensing laser source could be assembled in the same way as the optical input fiber using the folding interconnection technology. On the receiving side, a photodetector diode could directly be bonded to the backside output position. Also, the other essential parts can be integrated in a similar way, as done in other electronic watch like medical devices.

3. Dissemination material

To disseminate the pilot line capabilities, dissemination material from the model-case is prepared. In addition to this deliverable report, material includes flyer/brochure (Figure 19), one-slider for the pilot line Technical dissemination slide deck (Figure 20), model-case spread for the Handbook (Figure 21) and MedPhab web pages (Figure 22, Figure 23) that provides access to the handbook, flyer and model-case reports. In addition, two scientific papers are under preparation and will be used to dissemination once accepted.



Figure 19. A dissemination flyer/brochure “Wearable PIC temperature sensor” was compiled, with a technical title “Design, realization, characterization and proof of feasibility of a wearable temperature PIC sensor by linking capabilities at IMEC and CSEM SA”. Upper picture: Brochure front page and back page. Lower picture: Brochure inside spread.

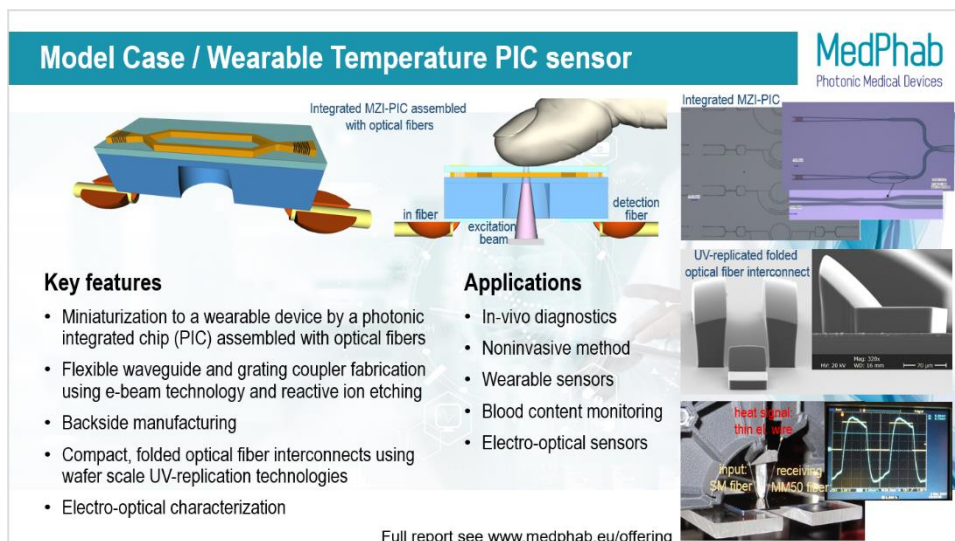


Figure 20 Model-case one-slider in the MedPhab Technical dissemination slide deck.

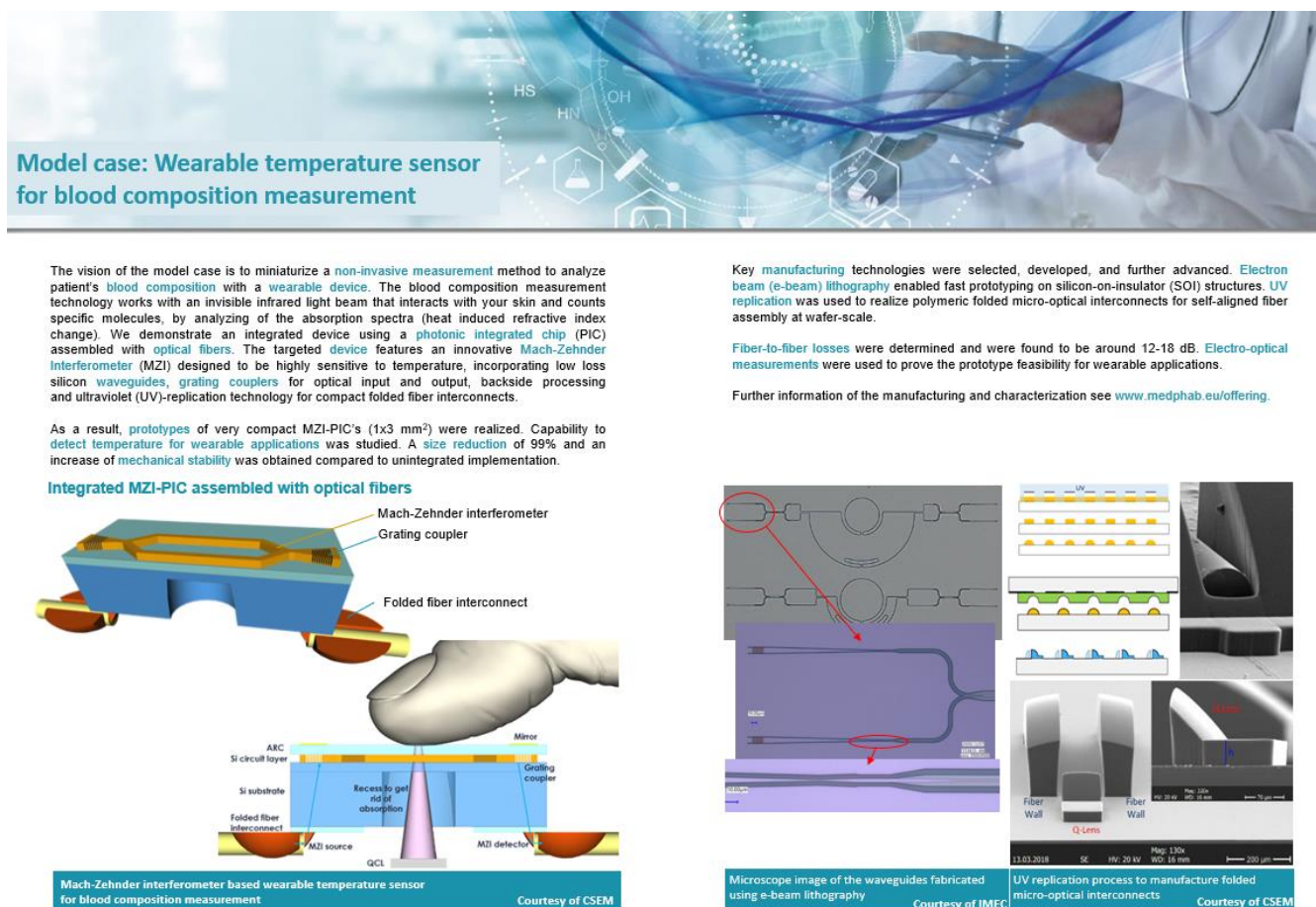


Figure 21. Draft of the model-case spread to be included to the next version of MedPhab Handbook.

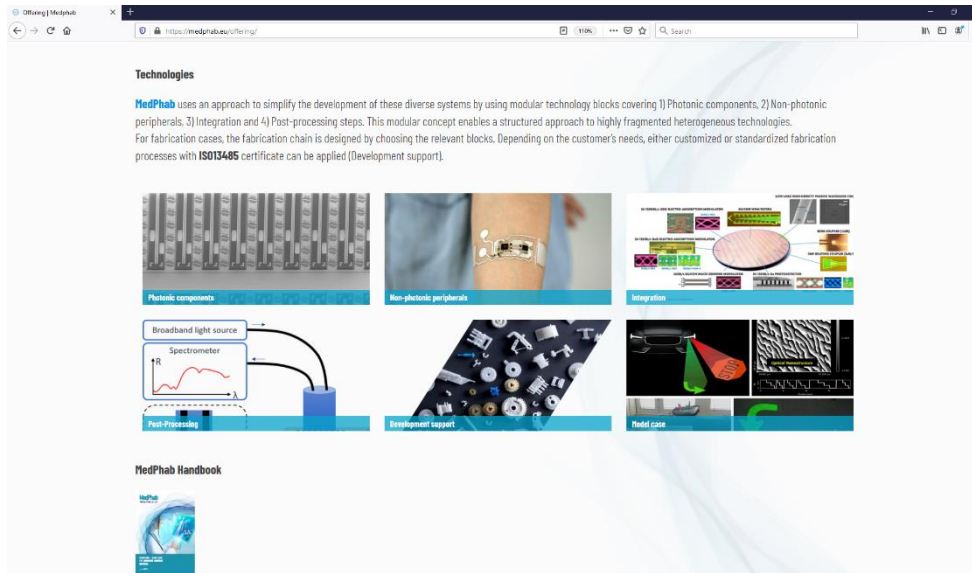


Figure 22. A screen capture image from the “Offering” page on the MedPhab’s webpages, showing the reserved slot for the model-cases, and the icon for downloading the MedPhab Handbook.

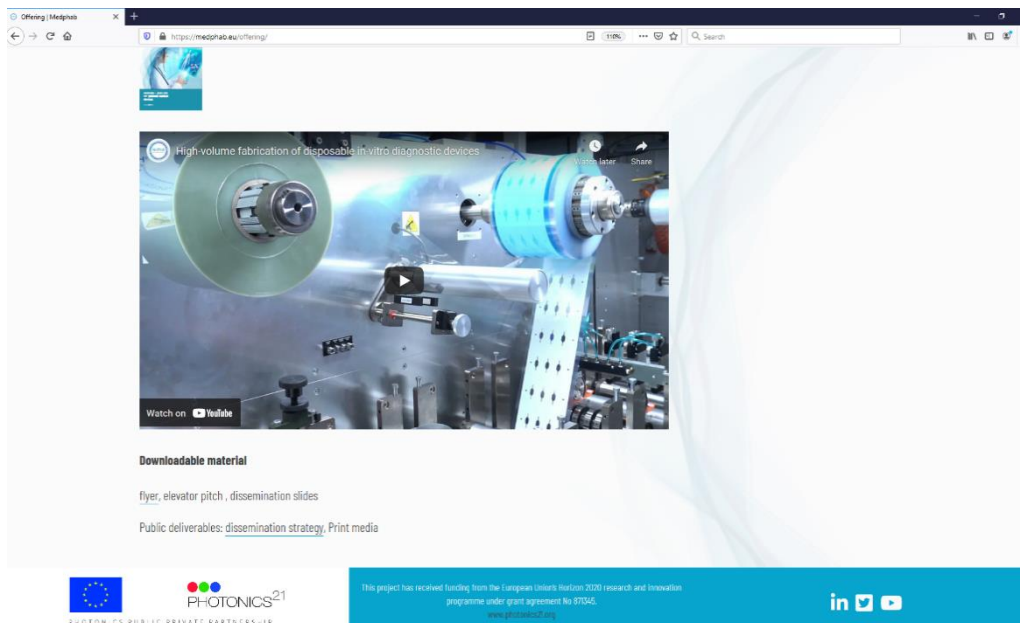


Figure 23. A screen capture image from the “Offering” page on the MedPhab’s webpages, showing the link to the Model case dissemination video material on MedPhab’s YouTube channel. Also links to other downloadable materials, such as flyers and dissemination slides, are shown.

The following scientific publications are under preparation:

1. MZI-PIC: Grigorij Muliuk, R. Krähenbühl, et. al; “Back-side, fiber-coupled, compact, fully-integrated MZI-PIC for temperature sensing applications”; to be published
2. Folded interconnect: R. Krähenbühl et. al; “Wafer-scale in-plane micro-optical interconnects for integrated photonics circuits (PICs)”; to be published

4. Conclusions

In this model-case, we presented the feasibility of MZI-PIC-based temperature sensor for wearable application. Two generations of Si waveguide/grating coupler devices were fabricated and delivered by IMEC to CSEM for further processing and electro-optical characterization. First, folded interconnect on top of gratings were realized and the devices were measured. Finally, the capability to detect temperature of the realized MZI-PIC was proofed.

The presented technologies are highly advantageous in prototyping of highly integrated and compact fiber assembled PICs. Furthermore, the implementation into high volume industrial production is straightforward, as all technologies are wafer level based.

5. Degree of Progress

The progress of the task with respect to the DoA is on target. The core activity was to develop dissemination material based on the model-case “Wearable temperature PIC sensor” (feasibility to develop a PIC-based temperature sensor for wearable applications). This deliverable is 100% fulfilled.

6. Dissemination Level

This deliverable is Public.